Hindawi
Advances in Materials Science and Engineering
Volume 2022, Article ID 3836863, 10 pages
https://doi.org/10.1155/2022/3836863

Research Article

Valorization of Water-Based Drill Cuttings through the Bio-Carbonation Approach

Guowang Tang,[1] **Feng Huang**,[1] **Guihe Wang**,[1] **Zhengyang Song**,[2] **Cangqin Jia**,[3] **Peizhi Yu**,[1] **and Yongshuai Sun**[4]

[1]*School of Engineering and Technology, China University of Geosciences, Beijing 100083, China*
[2]*Department of Civil Engineering, School of Civil & Resource Engineering, University of Science & Technology Beijing, Beijing 100083, China*
[3]*School of Engineering and Technology, China University of Geosciences and Key Laboratory of Deep Geodrilling Technology, Ministry of Land and Resources, Beijing 100083, China*
[4]*College of Water Resources & Civil Engineering, China Agricultural University, Beijing 100083, China*

Correspondence should be addressed to Feng Huang; huangfeng@cugb.edu.cn

Received 18 November 2021; Revised 8 January 2022; Accepted 16 April 2022; Published 6 May 2022

Academic Editor: Antonio Riveiro

This study proposed a novel bio-carbonation method to recycle water-based drill cutting (WDC) to prepare samples, which contains reactive magnesia (MgO) cement (RMC), ground granulated blast furnace slag (GGBS), and fly ash (FA), with the adoption of microbially induced carbonate precipitation (MICP). Through the investigation of some parameters (i.e., GGBS content, FA content, and curing time), the microstructures and strength development of bio-carbonated RMC-based WDC samples were evaluated. The preliminary results revealed that bio-carbonated RMC-based WDC samples outperformed the control group (i.e., without bio-carbonation) in terms of the 28-day strength (i.e., 9.8 MPa versus 4.4 MPa), which can be assigned to formation of the carbonates, that is, hydrated magnesium carbonates (HMCs). Further, in addition to the identification of HMCs, the microstructural analysis also revealed a continuous carbonate network due to the presence of HMCs, which accounts for the strength boost of samples.

1. Introduction

Drill cuttings, contaminated by drilling fluids, are soil-like waste, heterogeneous, and hazardous [1], and drilling fluids can lubricate and cool drilling tools. Meanwhile, they can stabilize the well bore and transport drill cuttings from well bores to the surface. Nevertheless, drilling fluids contain a certain percentage of heavy metals [2], water-soluble salts, and hydrocarbons [3, 4], which contaminate drill cuttings [5]. Due to the possible pollution, drilling cuttings are classified as a special waste by some countries such as US and Indonesia [6]. Hence, drill cuttings should be disposed of efficiently. Currently, according to the previous studies, there are various management options concerning drill cuttings, including the bioremediation [7], the thermal desorption [8], the disposal in landfills [9], the stabilisation/solidification [1], and the reuse in the construction sector [10, 11].

Amid the treatments as aforementioned, disposing drill cutting in landfills is feasible, as it enabled the contaminants to be metabolized, transformed, and assimilated by the microbial populations in soil [12]. At the same time, the thermal desorption is also employed to treat drill cuttings, which is supported by eliminating water, hydrocarbons [4], salinity, and clay, thereby retaining a relatively clean mixture [13, 14]. Meanwhile, in real engineering, treated drill cuttings can be reused as fillers in landfills and aggregates in concrete or brick [15]. It is to be mentioned that valorization of drill cuttings is considered to be efficient and economical. As previously reported by Asadi et al. [16], drill cuttings can be used to replace partial Portland cement (PC) [17–19], which is considered to be a major contributor to the global

greenhouse gas [20, 21]. Compared with PC, reactive magnesia (MgO) cement (RMC) is proposed recently as a sustainable construction material, which is extracted from seawater or brine (wet route) without the CO_2 emission [22]. Another advantage of RMC is that its low production temperature compared with that of PC (e.g., 700°C versus 1450°C) [23] and previous studies have confirmed that carbonated RMC could provide relatively great strength [24], and the reaction is that RMC first hydrates into brucite ($Mg(OH)_2$), and then it reacts with CO_2 to form various hydrated magnesium carbonates (HMCs) [23]. As a result, nesquehonite ($MgCO_3{\cdot}3H_2O$), hydromagnesite ($4MgCO_3{\cdot}Mg(OH)_2{\cdot}4H_2O$), dypingite ($4MgCO_3{\cdot}Mg(OH)_2{\cdot}5H_2O$), and artinite ($MgCO_3{\cdot}Mg(OH)_2{\cdot}3H_2O$) can be found in the specimens, which are identified as HMCs phases that are yielded from the carbonation process [25, 26].

To improve the mechanical properties of the carbonated RMC-based system, various supplementary cementitious materials including fly ash (FA) and ground granulated blast furnace slag (GGBS) [27] were used in mixtures, demonstrating that carbonated RMC-based mix incorporated with FA has been observed to enhance the agglomeration of carbonate samples, thereby forming more HMCs. Moreover, the formation of carbonate phases improved the morphology and interconnectivity of product phases [28]. In terms of GGBS, when it was involved in the carbonated RMC-based mixtures, the content of other hydration phases in the RMC-based system increased [29], where GGBS was activated with MgO, thus increasing the hydrotalcite content. As a consequence, the pore volume reduced that brought about improved strength. Meanwhile, the strength development was further improved in a CO_2-rich environment [30, 31].

A recent study also revealed that microbially induced carbonate precipitation (MICP) could be used to heal cracks in RMC-based systems [32] due to the formation of HMCs crystals that fill in the cracks via the bio-carbonation. To be more specific, in the MICP process, bacterial urease decomposes urea to provide carbonate ions, and then the ions react with Ca^{2+} to form $CaCO_3$ precipitates [33, 34, 35]. Similarly, Mg^{2+} (derived from the dissolution of RMC) was used to replace Ca^{2+}; thus, HMCs precipitates could be formed. The chemical reactions are shown in the following equations:

$$CO(NH_2)_2 + H_2O + \text{bacterialurease} \longrightarrow CO_3^{2-} + 2NH_4^+ \quad (1)$$

$$CO_3^{2-} + Mg^{2+} \longrightarrow MgCO_3\downarrow \quad (2)$$

Compared with RMC-based systems cured in a high concentration and pressure of CO_2, RMC-based MICP methods used urea as a carbonation source to eliminate the use of the high concentration of CO_2, which is more practical [24]. Moreover, most studies have explored the MICP process in a calcium-rich environment, so different from the conventional MICP process, the bio-carbonated RMC-based methods eliminate the use of calcium sources as an addition, which also reduces the cost of this approach.

This study innovatively investigates the microstructures and strength development of bio-carbonated RMC-based WDC samples containing GGBS and FA, and compared with carbonated RMC-based mixtures, a new bio-carbonated technology has been proposed to reuse WDCs. The strength and permeability of all samples were tested, facilitated by the uniaxial loading frame and the triaxial cell apparatus. Meanwhile, Fourier transform infrared spectroscopy (FTIR), X-ray diffraction (XRD), and scanning electron microscopy (SEM) were used to investigate the chemical compositions and the microstructures of the samples in details. The findings from this study revealed a new approach to effectively dispose of WDCs through the preparation of the bio-carbonation of RMC-based mixtures.

2. Material and Methods

2.1. Chemicals, Mixture Composition, and Sample Preparation. The *Sporosarcina pasteurii* (ATCC11859) strain was used for the preparation of bio-carbonated RMC-based WDC samples in this study. The bacteria were used to provide CO_2 to react with RMC to form HMCs in this study. The mother culture consisted of a mixture of soy peptone (5 g/L), casein peptone (15 g/L), urea (20 g/L), sodium chloride (5 g/L), and 1000 mL of deionized water. The pH value of the mother culture was about 7.3 and sterilized at 121°C for 30 minutes. The bacterial solution consisted of the mother culture and *Sporosarcina pasteurii*. The bacterial cultivation was carried out in 28°C, at a shaking rate of 160 rpm. For 36 hours, the bacterial solution was harvested. The originally harvested bacterial solution revealed the optical density (OD_{600}) of about 2 ± 0.1. Bacterial culture was used immediately after harvest and was not stored. Meanwhile, industrial grade urea was used.

RMC was supplied by the Japan Concorde Company and was analyzed via X-ray fluorescence spectrometry, and its chemical composition is listed in Table 1. WDCs were provided from a coal seam gas production block in Xinxiang, Henan, and their microstructure and chemical composition are revealed via SEM, FTIR, and XRD in Figures 1 and 2. Figure 1 shows flake amorphous WDC samples. Figure 2(a) displays the adsorption bands of samples. –OH group stretching vibrations were explained by peaks at 3,409 and 3,513 cm^{-1} [36]. The peaks at 871 and 712 cm^{-1} confirmed the presence of C-O. The peaks at 1,048, 798, 780, 526, and 470 cm^{-1} were attributed to many Si-O functional groups. The peaks at 2,925, 2857, 2,514, 1,795, and 1,396 cm^{-1} indicated the existence of C-O stretch. FTIR proved that $CaCO_3$ and SiO_2 were the main components of WDC. Figure 2(b) displays the XRD peaks of WDC samples, confirming the existence of $CaCO_3$ and SiO_2 inside the samples, which is in line with the FITR results. Fly ash (FA) and ground granulated blast furnace slag (GGBS) were obtained from Boheng mineral products trading Co., Ltd. Their chemical compositions are shown in Figure 3. GGBS and FA were composed of glassy phases and mullite ($3Al_2O_3.2SiO_2$), respectively.

2.2. Bio-Carbonation of RMC-Based WDC Samples. Bio-carbonated RMC-based WDC samples were prepared by stirring the mixtures (i.e., WDCs, FA, GGBS,

Table 1: Chemical composition of RMC.

Chemical composition (%)						
MgO	CaO	SiO_2	Fe_2O_3	Al_2O_3	MnO	Others
96.142	1.791	0.863	0.324	0.057	0.035	0.789

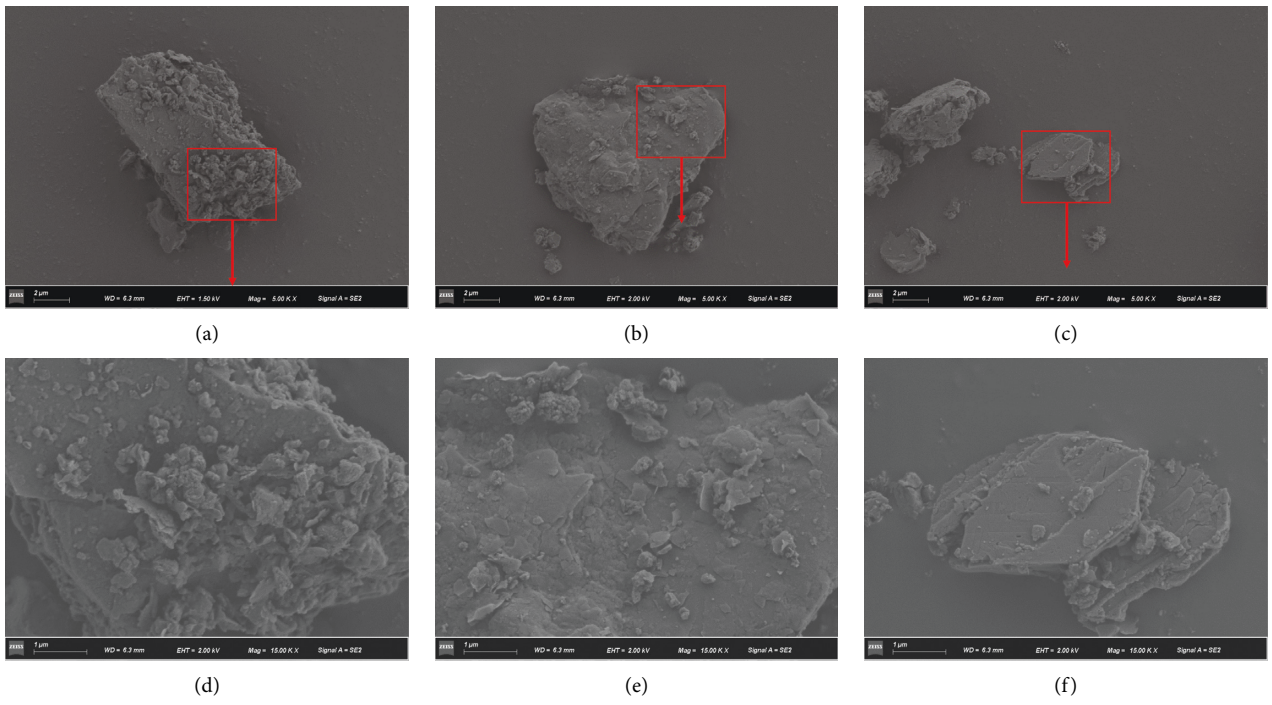

Figure 1: SEM images of WDC samples.

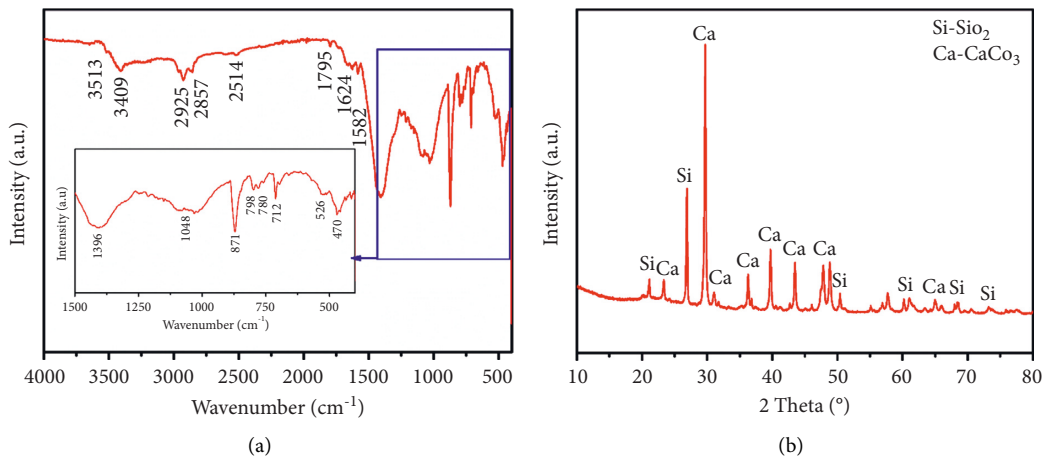

Figure 2: FTIR and XRD pattern of WDC samples.

and RMC) for 2 mins, then followed by the addition of bacterial solution or water. The solid and liquid mixture was stirred for another 1 min. The freshly prepared mixture was cast into $50 \times 50 \times 50$ mm cubes and finished with a trowel. All samples were demoulded after 24 h and cured under an ambient temperature ($30 \pm 1.5^{\circ}C$) and relative humidity ($20 \pm 5\%$) to improve strength for up to 28 days.

RMC content was mixed with 20 wt. % of WDC. Three different FA concentrations (5%, 15%, and 25%) and GGBS concentrations (10%, 20%, and 30%) were studied by the WDC weight. Water content (i.e., water/solid: 30%) referred to the quality of bacterial solution was used in this study. All mixture formulations are listed in Table 2, and 9 samples were cast for each mixture under different curing durations at 7, 14, and 28 days. For control samples, the same quality of

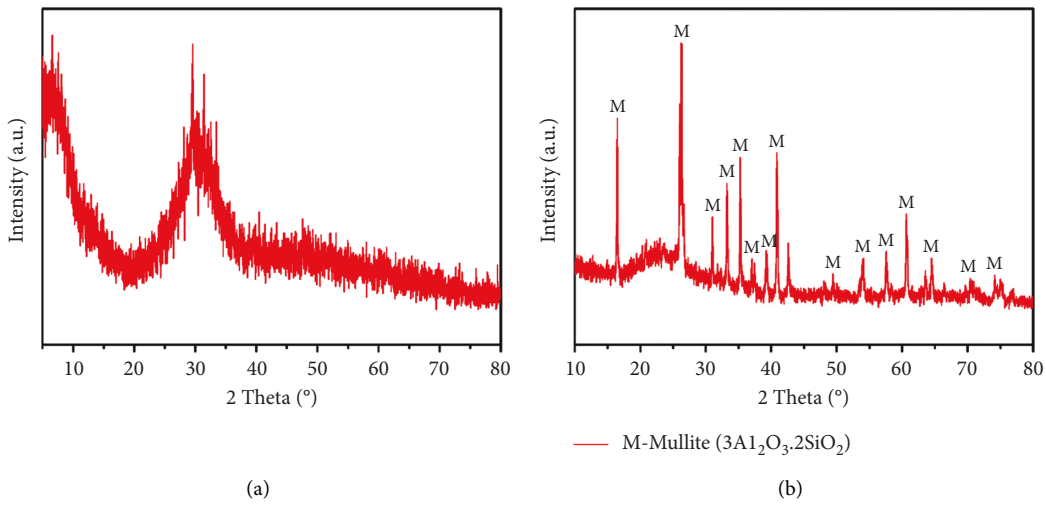

Figure 3: XRD pattern of GBS and FA samples.

Table 2: Mixture formulations prepared under this study.

Sample	Mix composition					Curing conditions
	Sand (g)	RMC (g)	GGBS (g)	FA (g)	Water content (30%)	
0	600	120	180	30	Deionized water	Air
1	600	120	60	30	Bacterial solution	Air
2	600	120	60	60	Bacterial solution	Air
3	600	120	60	90	Bacterial solution	Air
4	600	120	120	30	Bacterial solution	Air
5	600	120	120	60	Bacterial solution	Air
6	600	120	120	90	Bacterial solution	Air
7	600	120	180	30	Bacterial solution	Air
8	600	120	180	60	Bacterial solution	Air
9	600	120	180	90	Bacterial solution	Air

deionized water was used to replace bacterial culture, whose details are presented in Table 2 (i.e., Sample 0).

2.3. UCS and Permeability Tests. According to ASTM D2166/D2166M [37, 38], the strength of all samples were measured with an uniaxial loading frame. After 7, 14, and 28 days of curing, the compression test was performed at a loading rate of 1 mm/min. The permeability coefficient of all samples was also tested by the water drive with a triaxial cell apparatus [39]. The confining pressure of 3 MPa was applied to the samples, and the pressure difference was from 0 to 6 MPa. All sampling was carried out in triplicate to obtain the standard deviations.

2.4. SEM, FTIR, and XRD Analyses. Fragments extracted from UCS testing were dried for 24 h, and then they were ground into powders. The powder sample passed through a sieve size of 75 mm before FTIR, XRD, and SEM analyses. The XRD measurement was performed with an automatic XRD instrument (Brooke, Germany). The scanning speed was 0.15 s $step^{-1}$, and the range of 2θ is 10°~80°. The FTIR data were collected with an infrared spectrometer (FTIR8400, SHIMADZU, Japan) with a wavenumber range of 4000–400 cm^{-1}, and the scanning times and resolution is 32 4 cm^{-1}, respectively. The morphologies of the RMC-based WDC samples and bio-carbonated RMC-based WDC samples were investigated using a scanning electron microscopy (SEM, Zeiss Supra 55, Germany) with an acceleration voltage of 25 kV.

3. Results and Discussion

3.1. Strength and Permeability. Figure 4 presents the UCS of all samples after curing 7, 14, and 28 day. Compared with sample 0 and sample 8, the strength of sample varied from 4.4 to 9.8 MPa after 28 days of curing, which proved that bio-carbonated RMC-based samples was effective to treat WDC. It was worth mentioning that the maximum strength of samples reached 6.9 MPa after 7 days of curing, indicating a faster strength gain at an early age. Meanwhile, previous studies reported that urea was completely hydrolyzed to form carbonate ions by MICP in 1 day, and through the reaction between carbonate ions and brucite ($Mg(OH)_2$), the formed HMCs enhanced strength of bio-carbonated RMC-based WDC samples at early age [40]. In addition, it was observed that the strength of bio-carbonated RMC-based samples increased over time from 7 to 28 days, thereby highlighting the continuation of the hydration and carbonation process [41]. This was mainly because the available

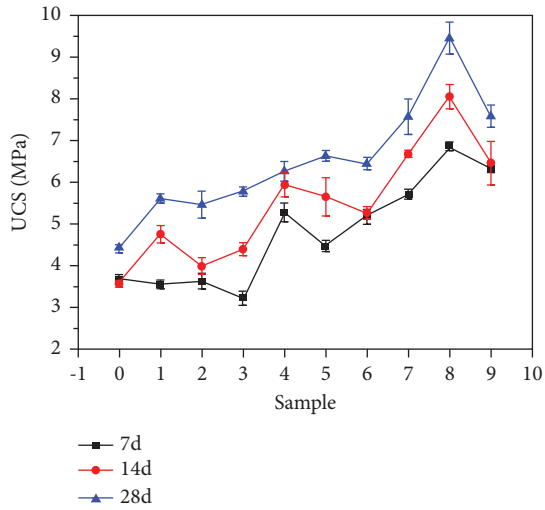

Figure 4: UCS of bio-carbonated RMC-based WDC samples.

unreacted RMC in the samples continuously hydrated and transformed into $Mg(OH)_2$ during the curing process, thereby reacting with carbonate ions to form more HMCs that contributes to the further strength development after 28 day of curing.

Figure 4 also shows the effects of GGBS and FA concentrations on the strength of bio-carbonated RMC-based WDC samples. Compared with samples 2, 5, and 8 after 28 days of curing, the strength of bio-carbonated samples increased from 5.5 to 9.5 MPa when GGBS content increased from 10 to 30%. This was because GGBS has been activated by RMC, and the content of hydrotalcite increased in samples, thereby reducing the pore volume and enhancing the strength development of bio-carbonated samples [42]. The strength of samples was further improved via the bio-carbonated process due to the formation of different carbonate phases [30, 31], explaining their greater strength. When GGBS was 60 g and 120 g, the lower strength of bio-carbonated samples could be observed with an increase in FA concentrations. Nevertheless, 60 grams of FA achieved the maximum strength when GGBS concentration was 180 grams in the samples. This was because the addition of FA was considered to enhance the pozzolanic reaction and yield more hydrate phases (e.g., M-S-H and hydrotalcite), thus reducing the pore volume and elevating the strength of samples. However, the above results also confirmed that the mix design was important. In terms of the permeability, the initial permeability of pure WDC column was $1.1 \pm 2 \times 10^{-2}$ m/s without the confining pressure, while the permeability test showed that the permeability coefficient of all bio-carbonated RMC-based WDC samples and sample 0 was 0 cm/s, indicating the large bio-carbonation extent of samples, where the pore space was reduced with the formation of HMCs.

3.2. FTIR. Figure 5 depicts the FTIR spectra of bio-carbonated RMC-based WDC samples within various GGBS and FA concentrations after 28 days of curing. The molecular groups of the samples within various GGBS and FA concentrations were found to be similar. In all samples, the peak at 3,697 cm^{-1} indicated the presence of the O-H functional groups, which was formed by the hydration of RMC that led to the formation of $Mg(OH)_2$ [43]. The peak of 565 cm^{-1} was assigned to the presence of MgO [44]. The above results showed the presence of unreacted MgO and $Mg(OH)_2$, thereby confirming the incomplete hydration and carbonation. The peaks of 1463 cm^{-1} with an asymmetric stretch were attributed to the present of C-O stretch, which further proved the formation of HMCs [44, 45]. The peaks of 870 and 712 cm^{-1} with a bending vibration also proved the existence of C-O [46]. Furthermore, a higher carbonation band intensity was observed with an increase in GGBS concentrations, which indicated the increased formation of carbonate phases [27]. Nevertheless, the carbonation band intensity decreased when FA concentrations increased. This proved that the strength development of samples was associated with the carbonate phase contents. The peaks at 1,058 cm^{-1} were attributed to the existence of Al-O bending, which was associated with the hydrotalcite formed with FA and GGBS [27]. The characteristic peak at 1,720 and 3,122 cm^{-1} can be assigned to the existence of O-H bending, which was associated with the M-S-H formed within FA [46, 47].

3.3. XRD. Figure 6 displays the XRD patterns of bio-carbonated RMC-based WDC samples within various GGBS and FA concentrations after 28 days of curing. The peak positions of all samples within various GGBS and FA concentrations were found to be similar. Among some peaks of the samples, the diffraction peaks of MgO (at 43° and 62° 2θ) and brucite (at 18.6°, 38°, 50.8°, and 68.2°2θ) were observed, which were consistent with the FTIR outcomes. Meanwhile, unreacted MgO and brucite confirmed incomplete hydration and carbonation over time, indicating the prospect of bio-carbonated approach to further facilitate the strength development if the complete hydration and carbonation in the samples were to be achieved.

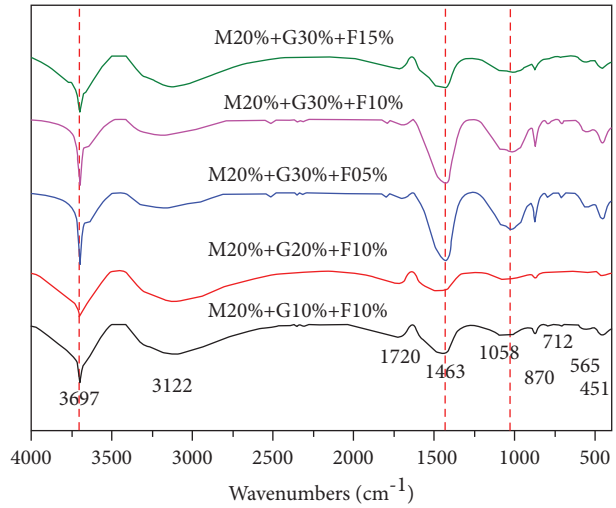

Figure 5: FTIR pattern of bio-carbonated RMC-based WDC samples after 28 days of curing.

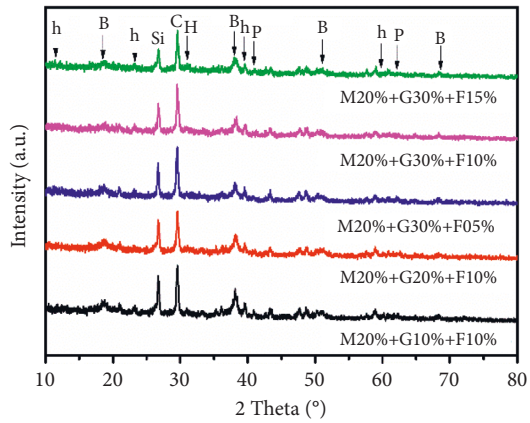

Figure 6: XRD pattern of bio-carbonated RMC-based WDC samples after 28 days of curing (h: hydrotalcite; H: hydromagnesite; B: brucite; P: MgO; C: $CaCO_3$; Si: SiO_2).

The broad peaks (at 10–25°, 32–37°, and 56–65° 2θ) were attributed to the existence of amorphous M-S-H [48], which were observed in all samples since hydration occurred in the present of water. Meanwhile, the peaks of hydrotalcite were also observed at 12.1°, 23°, and 61° 2θ. Furthermore, the main peak of hydromagnesite was observed at around 30.6° 2θ. The existence of M-S-H, hydrotalcite, and hydromagnesite was an indication of the occurrence of hydration and bio-carbonation simultaneously over time. These observations were in agreement with the strength development, highlighting the effectiveness of strength improvement via bio-carbonation.

3.4. SEM. Figure 7 shows the SEM images of RMC-based WDC samples. WDC particles were surrounded with hydration products, as shown in Figure 7(a). This was because the hydrated phases were initially formed onto the WDC particle surface and acted as the nucleation sites of hydrolysis process; thus, the WDC particles were surrounded with the reduced porosity and the boost of strength development, which was consistent with previous studies [27]. Figures 7(c) and 7(d) present morphologies of packed M-S-H structures and hydrotalcite (i.e., hydration phases), which is as a result of the hydration of MgO and SiO_2 [27]. Moreover, the addition of GGBS into the bio-carbonated RMC-based samples elevated the solubility of glassy phases, consequently achieving the formation of hydrotalcite in the samples.

Figure 8 exhibits SEM images of bio-carbonated RMC-based WDC samples. Unlike the RMC-based WDC samples, the microstructural development of bio-carbonated RMC-based WDC samples was controlled with the formation of carbonate phases (e.g., hydromagnesite). Figures 8(c) and 8(d) show the widespread presence of rosette-like crystals, which are identified as the hydromagnesite [49]. Meanwhile, compared with morphologies of RMC-based WDC samples, bio-carbonated RMC-based WDC samples presented denser inner structures (Figures 7(a) and 7(b)) owing to the formation of carbonate phases, which reduced the pore volume and formed a continuous carbonate network, facilitating the strength development. Overall, the microstructural

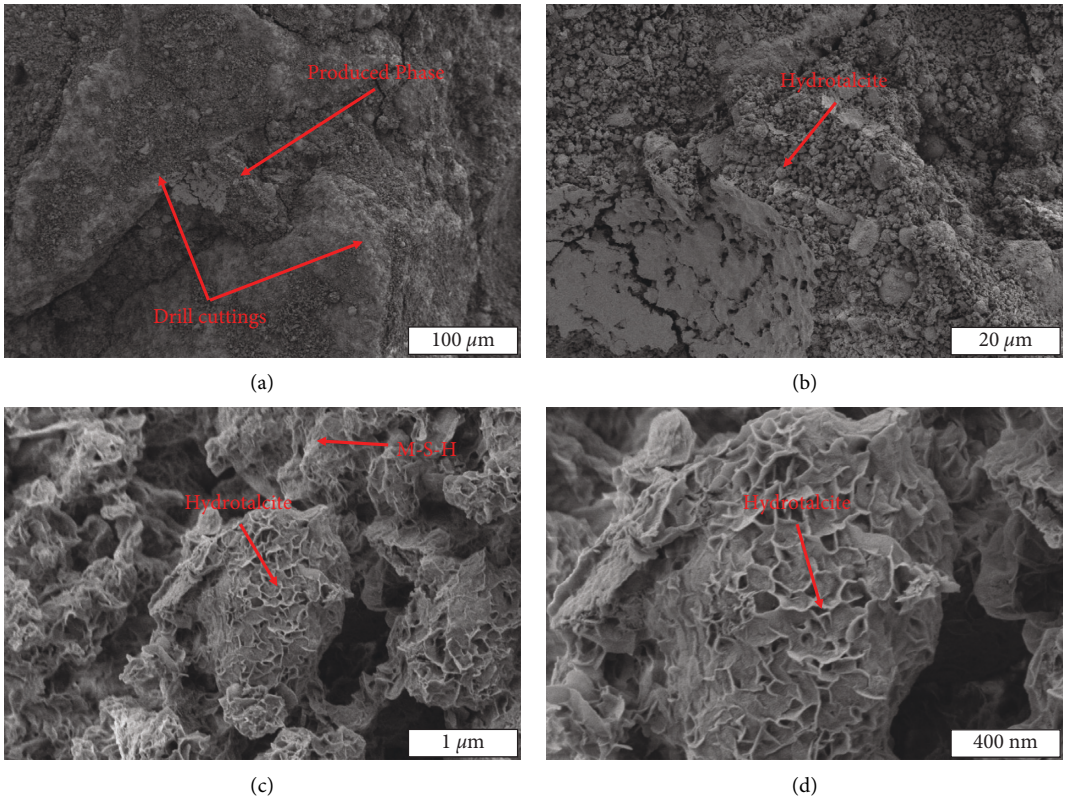

Figure 7: SEM images of the RMC-based WDC samples after 28 days of curing.

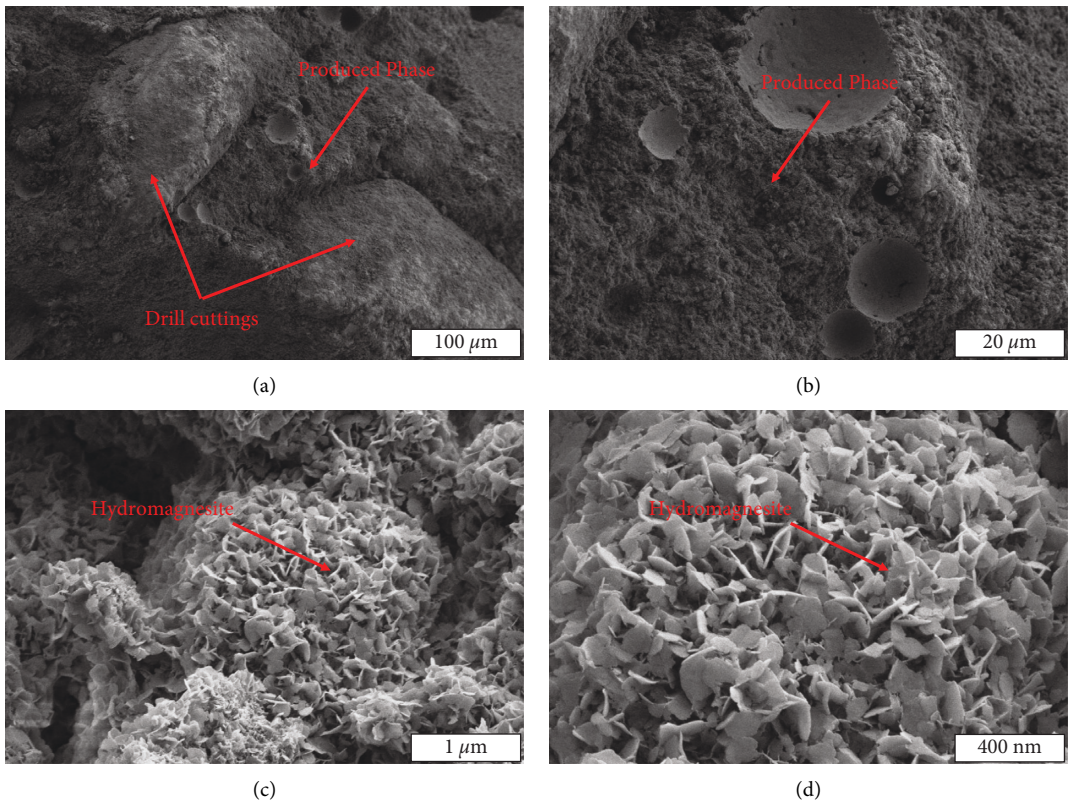

Figure 8: SEM images of bio-carbonated RMC-based WDC samples after 28 days of curing.

development was in agreement with the FTIR and XRD results, and they can account for the strength development of the samples.

4. Conclusion

The study aimed to investigate the use of MICP to valorize RMC-based WDC, where the relationship between the strength and microstructural development of the samples containing GGBS and FA was studied. While RMC-based WDC samples obtained the strength with the formation of M-S-H and hydrotalcite in the existence of GGBS and FA, bio-carbonated RMC-based WDC samples gained higher strength owing to the formation of an additional continuous carbonate (e.g., HMCs) network.

The strength of bio-carbonated samples increased from 5.5 to 9.8 MPa in the GGBS content from 10 to 30%, which indicated GGBS was a suitable additive in terms of the strength development. When the concentration of FA is 60 g, this was considered to be the optimal dosage. In terms of the optimal formulation (sample 8), the strength of sample revealed was up to 9.8 MPa after 28 days of curing. Therefore, the mix design of bio-carbonated RMC-based samples should be further optimized to enhance the strength development and microstructure refinement.

Overall, this study concluded that the optimum mix composition of bio-carbonated RMC-based WDC samples was 20% of RMC, 30% of GGBS, and 10% of FA at a w/s of 30%, highlighting the effectiveness of a new method for the treatment of valorization of WDC, that is, through the preparation of bio-carbonated RMC-based mixtures.

Data Availability

Some or all data, models, or code that support the findings of this study are available from the corresponding author upon reasonable request.

Disclosure

Yongshuai Sun is the co-first author.

Conflicts of Interest

This is a submission from one of the editorial board of the special issue (zhengyang song). The authors declare that they have no conflicts of interest to this work. The authors declare that they do not have any commercial or associative interest that represents conflicts of interest in connection with the work submitted.

Acknowledgments

This work was supported by the Beijing Natural Science Foundation (8214060), the National Natural Science Foundation of China (41772388), the National Natural Science Foundation of China (42107164), the National Natural Science Foundation of China (51991364 and 41807230), the Fundamental Research Funds for the Central Universities (2–9-2018–090), and the Research Foundation of Key Laboratory of Deep Geodrilling Technology, Ministry of Natural Resources (PY201904).

References

[1] M. S. Al-Ansary and A. Al-Tabbaa, "Stabilisation/solidification of synthetic petroleum drill cuttings," *Journal of Hazardous Materials*, vol. 141, no. 2, pp. 410–421, 2007.

[2] T. Yang and J. Zhang, "Research on the treatment technology of soft rock floor heave based on a model of pressure-relief slots," *Arabian Journal of Geosciences*, vol. 14, no. 13, p. 1278, 2021.

[3] S. A. Leonard and J. A. Stegemann, "Stabilization/solidification of petroleum drill cuttings: leaching studies," *Journal of Hazardous Materials*, vol. 174, no. 1-3, pp. 484–491, 2010.

[4] Z. Li, Y. Zhou, X. Meng, and S. Wang, "Harmless and efficient treatment of oily drilling cuttings," *Journal of Petroleum Science and Engineering*, vol. 202, Article ID 108542, 2021.

[5] B. Zhou, B. Lei, L. Hou, L. Huang, X. Lian, and B. Zhou, "Research on the harmless and recycling treatment technology of drilling waste mud based on changqing oilfield," *IOP Conference Series: Earth and Environmental Science*, vol. 804, no. 2, Article ID 022106, 2021.

[6] R. B. Kogbara, B. B. Dumkhana, J. M. Ayotamuno, and R. N. Okparanma, "Recycling stabilised/solidified drill cuttings for forage production in acidic soils," *Chemosphere*, vol. 184, pp. 652–663, 2017.

[7] C.-H. Chaineau, J.-L. Morel, and J. Oudot, "Microbial degradation in soil microcosms of fuel oil hydrocarbons from drilling cuttings," *Environmental Science & Technology*, vol. 29, no. 6, pp. 1615–1621, 1995.

[8] J. P. Robinson, S. W. Kingman, and O. Onobrakpeya, "Microwave-assisted stripping of oil contaminated drill cuttings," *Journal of Environmental Management*, vol. 88, no. 2, pp. 211–218, 2008.

[9] J. Veil, D. Elcock, M. Raivel, C. Dan, and B. Grunewald, "Disposal of nonhazardous oil field wastes into salt caverns," in *Proceedings of the ., SPE Health, Safety and Environment in Oil and Gas Exploration and Production Conference*, New Orleans, Louisiana, June 1996.

[10] B. Ayati, C. Molineux, D. Newport, and C. Cheeseman, "Manufacture and performance of lightweight aggregate from waste drill cuttings," *Journal of Cleaner Production*, vol. 208, no. 1-1658, pp. 252–260, 2019.

[11] Z. Song, H. Konietzky, and M. Herbst, "Bonded-particle model-based simulation of artificial rock subjected to cyclic loading," *Acta Geotechnica*, vol. 14, no. 4, pp. 955–971, 2019.

[12] S. I. Onwukwe and M. S. Nwakaudu, "Drilling wastes generation and management approach," *International Journal of Environment and Sustainable Development*, vol. 3, no. 3, pp. 252–257, 2012.

[13] E. Ifeadi, "The treatment OF drill cuttings using dispersion BY chemical reaction (dcr)," in *Proceedings of the A paper prepared for presentation at the DPR Health, Safety & Environment (HSE) International Conference on Oil and Gas Industry in Port Harcourt*, Nigeria, 2004.

[14] A. Gma and B. Ipj, "Microwave remediation of oil-contaminated drill cuttings – a review," *Journal of Petroleum Science and Engineering*, vol. 207, 2021.

[15] B. Mohammed and C. R. Cheeseman, "Use of oil drill cuttings as an alternative raw material in sandcrete blocks," *Waste and Biomass Valorization*, vol. 2, no. 4, pp. 373–380, 2011.

[16] E. Mostavi, S. Asadi, and E. Ugochukwu, "Feasibility study of the potential use of drill cuttings in concrete," *Procedia Engineering*, vol. 118, no. 6, pp. 1015–1023, 2015.

[17] M. Foroutan, M. M. Hassan, N. Desrosiers, and T. Rupnow, "Evaluation of the reuse and recycling of drill cuttings in concrete applications," *Construction and Building Materials*, vol. 164, pp. 400–409, 2018.

[18] L. Yu, L. Fang, P. Zhang, S. Zhao, B. Jiao, and D. Li, "The utilization of alkali-activated lead-zinc smelting slag for chromite ore processing residue solidification/stabilization," *International Journal of Environmental Research and Public Health*, vol. 18, no. 19, p. 9960, 2021.

[19] L. Calgaro, S. Contessi, A. Bonetto et al., "Calcium aluminate cement as an alternative to ordinary Portland cement for the remediation of heavy metals contaminated soil: mechanisms and performance," *Journal of Soils and Sediments*, vol. 21, no. 4, pp. 1755–1768, 2021.

[20] J. Qiu, S. Ruan, C. Unluer, and E.-H. Yang, "Autogenous healing of fiber-reinforced reactive magnesia-based tensile strain-hardening composites," *Cement and Concrete Research*, vol. 115, pp. 401–413, 2019.

[21] Z. Song, T. Frühwirt, and H. Konietzky, "Inhomogeneous mechanical behaviour of concrete subjected to monotonic and cyclic loading," *International Journal of Fatigue*, vol. 132, no. Mar, pp. 105381–105383, 2020.

[22] H. Dong, C. Unluer, E.-H. Yang, and A. Al-Tabbaa, "Synthesis of reactive MgO from reject brine via the addition of NH4OH," *Hydrometallurgy*, vol. 169, pp. 165–172, 2017.

[23] S. Ruan and C. Unluer, "Comparative life cycle assessment of reactive MgO and Portland cement production," *Journal of Cleaner Production*, vol. 137, no. 20, pp. 258–273, 2016.

[24] X. Xiao, L. X. Goh, C. Unluer, and E.-H. Yang, "Bacteria-induced internal carbonation of reactive magnesia cement," *Construction and Building Materials*, vol. 267, Article ID 121748, 2021.

[25] M. Liska and A. Al-Tabbaa, "Performance of magnesia cements in porous blocks in acid and magnesium environments," *Advances in Cement Research*, vol. 24, no. 4, pp. 221–232, 2012.

[26] S. Ruan and C. Unluer, "Influence of mix design on the carbonation, mechanical properties and microstructure of reactive MgO cement-based concrete," *Cement and Concrete Composites*, vol. 80, pp. 104–114, 2017.

[27] S. Kumar, C. Sonat, E.-H. Yang, and C. Unluer, "Performance of reactive magnesia cement formulations containing fly ash and ground granulated blast-furnace slag," *Construction and Building Materials*, vol. 232, Article ID 117275, 2020.

[28] L. Mo, F. Zhang, D. K. Panesar, and M. Deng, "Development of low-carbon cementitious materials via carbonating Portland cement-fly ash-magnesia blends under various curing scenarios: a comparative study," *Journal of Cleaner Production*, vol. 163, no. oct.1, pp. 252–261, 2017.

[29] L. Pu and C. Unluer, "Durability of carbonated MgO concrete containing fly ash and ground granulated blast-furnace slag," *Construction and Building Materials*, vol. 192, no. DEC.20, pp. 403–415, 2018.

[30] D. K. Panesar and L. Mo, "Properties of binary and ternary reactive MgO mortar blends subjected to CO2 curing," *Cement and Concrete Composites*, vol. 38, no. Complete, pp. 40–49, 2013.

[31] M. B. Haha, B. Lothenbach, G. Le Saout, and F. Winnefeld, "Influence of slag chemistry on the hydration of alkali-activated blast-furnace slag - Part I: e," *Cement and Concrete Research*, vol. 41, no. 9, pp. 955–963, 2011.

[32] S. Ruan, J. Qiu, Y. Weng, Y. Yang, E. H. Yang, and J. Chu, "The use of microbial induced carbonate precipitation in healing cracks within reactive magnesia cement-based blends," *Cement and Concrete Research*, vol. 115, pp. 176–188, 2019.

[33] G. Tang, G. Wang, Y. An, and H. Zhang, "Graphene oxide on microbially induced calcium carbonate precipitation," *International Biodeterioration & Biodegradation*, vol. 145, Article ID 104767, 2019.

[34] G. Amarakoon and S. Kawasaki, "Factors affecting sand solidification using MICP with pararhodobacter sp," *Materials Transactions*, vol. 59, no. 1, pp. 72–81, 2018.

[35] N. Kazunori, F. Masahiro, T. Momoko, and K. Satoru, "Effects of Cationic Polypeptide on CaCO 3 Crystallization and Sand Solidification by Microbial-Induced Carbonate Precipitation," *Acs Sustainable Chemistry & Engineering*, vol. 6, 2018.

[36] S. Zhan, Y. Yang, Z. Shen et al., "Efficient removal of pathogenic bacteria and viruses by multifunctional amine-modified magnetic nanoparticles," *Journal of Hazardous Materials*, vol. 274, pp. 115–123, 2014.

[37] ASTM, "Standard Test Method for Compressive Strength of Hydraulic Cement Mortars," 2013, https://www.astm.org/c0109_c0109m-20.html.

[38] Z. Song, Y. Wang, H. Konietzky, and X. Cai, "Mechanical behavior of marble exposed to freeze-thaw-fatigue loading," *International Journal of Rock Mechanics and Mining Sciences*, vol. 138, Article ID 104648, 2021.

[39] V. Drnevich and R. W. Stephenson, "Permeability testing in the triaxial cell," *Geotechnical Testing Journal*, vol. 9, no. 1, pp. 3–9, 1986.

[40] Y. Yang, J. Chu, Y. Xiao, H. Liu, and L. Cheng, "Seepage control in sand using bioslurry," *Construction and Building Materials*, vol. 212, pp. 342–349, 2019.

[41] M. A. Shand, *The Chemistry and Technology of Magnesia*, wiley, Hoboken, New Jersey, USA, 2006.

[42] J. I. Escalante-Garcia, L. J. Espinoza-Perez, A. Gorokhovsky, and L. Y. Gomez-Zamorano, "Coarse blast furnace slag as a cementitious material, comparative study as a partial replacement of Portland cement and as an alkali activated cement," *Construction and Building Materials*, vol. 23, no. 7, pp. 2511–2517, 2009.

[43] C. Sonat, N. T. Dung, and C. Unluer, "Performance and microstructural development of MgO–SiO 2 binders under different curing conditions," *Construction and Building Materials*, vol. 154, pp. 945–955, 2017.

[44] R. L. Frost, S. J. L. Palmer, and S. J. Palmer, "Infrared and infrared emission spectroscopy of nesquehonite Mg(OH)(HCO3).2H2O-implications for the formula of nesquehonite," *Spectrochimica Acta Part A: Molecular and Biomolecular Spectroscopy*, vol. 78, no. 4, pp. 1255–1260, 2011.

[45] R. L. Frost and J. T. Kloprogge, "Infrared emission spectroscopic study of brucite," *Spectrochimica Acta Part A: Molecular and Biomolecular Spectroscopy*, vol. 55, no. 11, pp. 2195–2205, 1999.

[46] C. Kuenzel, F. Zhang, V. Ferrándiz-Mas, C. R. Cheeseman, and E. M. Gartner, "The mechanism of hydration of MgO-hydromagnesite blends," *Cement and Concrete Research*, vol. 103, pp. 123–129, 2018.

[47] P. Nath and P. Sarker, "Effect of fly ash on the durability properties of high strength concrete," *Procedia Engineering*, vol. 14, no. 3, pp. 1149–1156, 2011.

[48] Tonelli, C. Martini, G. Fratini, Ridi, Borsacchi, and Baglioni, *Structural characterization of magnesium silicate hydrate: towards the design of eco-sustainable cements*, Dalton Transactions, Cambridge, England, 2016.

[49] S. Ruan and C. Unluer, "Influence of supplementary cementitious materials on the performance and environmental impacts of reactive magnesia cement concrete," *Journal of Cleaner Production*, vol. 159, no. aug.15, pp. 62–73, 2017.